NANO LETTERS

2007
Vol. 7, No. 8
2276−2280

Electrically Excited Infrared Emission from InN Nanowire Transistors

Jia Chen,*,† Guosheng Cheng,‡ Eric Stern,§ Mark A. Reed,‡,|| and Phaedon Avouris†

IBM T. J. Watson Research Center, Yorktown Heights, New York 10598, Departments of Electrical Engineering, Biomedical Engineering, and Applied Physics, Yale University, New Haven, Connecticut 06520

Received April 11, 2007; Revised Manuscript Received May 28, 2007

ABSTRACT

We report electrically excited infrared emission from a single InN nanowire transistor. We report on: (1) the generation of IR emission by impact excitation of carriers under a high electrical field, (2) the size of the fundamental band gap of InN NW by measuring its emission spectra, (3) the observation of interband and conduction-band to conduction-band hot-carrier emission, and the carrier relaxation rate, and finally, (4) we present evidence that suggests that the electron accumulation layer at the InN NW surface forms a surface plasmon that couples to and enhances radiative electron–hole pair recombination.

In the past few years, we have seen intense interest focused on inorganic nanowires (NWs) and their properties.[1−9] Particular emphasis has been placed on the photonic and opto-electronic properties of NWs.[1−9] Lasing from individual NWs,[2−3] electrically induced emission from NW−NW contacts,[4−5] and electroluminescence[5−7] have been reported. However, not many NWs are found to luminescence because of surface and bulk traps that lead to nonradiative decay of the excitons.

Semiconducting group III nitrides have been the focus of much research in recent years because of their excellent inherent electronic and optoelectronic properties. In particular, indium nitride (InN) was predicted to have the lowest effective electron mass among all the III−nitride compounds, potentially leading to a high mobility semiconductor.[10] In addition, InN has an unexpectedly low band gap of 0.7−0.9 eV,[11] rather than 1.8−2.1 eV as previously believed,[10] so that it emits in the wavelength range of 1−2 μm, which is widely used by the telecommunication industry. Such emission can extend the range of nitride-based LEDs from ultraviolet (UV) to infrared (IR), and the band gaps of alloys of indium nitride—such as indium gallium nitride—can span the entire solar spectrum, leading to a wide range of potential optoelectronics applications.

In this work, we report the first study of *electrically excited* infrared (IR) emission from a single InN nanowire (NW). We demonstrate efficient generation of IR emission through impact excitation by hot carriers under a high applied electric field. The emission intensity increases exponentially with the drive current. We spectrally resolve the emission and show that it involves strong interband and conduction-band to conduction-band hot-carrier transitions. The spectra give a band gap of the electroluminescent InN NWs that agrees well with that measured using photoluminescence (PL) techniques. Most importantly, we discuss the formation of a surface plasmon from the intrinsic electron accumulation layer at the InN NW surface, and its possible role in the enhancement of the radiative electron−hole pair recombination.

Being a strongly polar semiconductor, InN has a unique band structure. In wurtzite-type InN, the conduction-band minimum at the center of the Brillouin zone (Γ point) is at much lower energy compared with the rest of the conduction-band edge.[12] As a result, the charge neutrality level is quite high in the conduction-band at the Γ point, leading to the observed high unintentional n-type doping, positively charged donor-type states, and an electron accumulation layer at the surface.[13] This intrinsic electron accumulation layer at wurtzite InN surfaces, with a density significantly higher than in any other of the III−V semiconductors, has been substantiated by a number of experimental techniques.[13−16] For example, Hall measurements of the sheet carrier density as a function of InN film thickness and capacitance−voltage ($C-V$) profiling have indicated the existence of an excess sheet electron density along its surface.[14] Valence-band X-ray photoelectron spectroscopy (XPS) revealed that the InN surface Fermi level lies at 1200−1600 meV above the

* To whom correspondence should be addressed. E-mail: chenjia@us.ibm.com.
† IBM T. J. Watson Research Center.
‡ Department of Electrical Engineering, Yale University.
§ Department of Biomedical Engineering, Yale University.
|| Department of Applied Physics, Yale University.

10.1021/nl070852y CCC: $37.00
Published on Web 07/07/2007

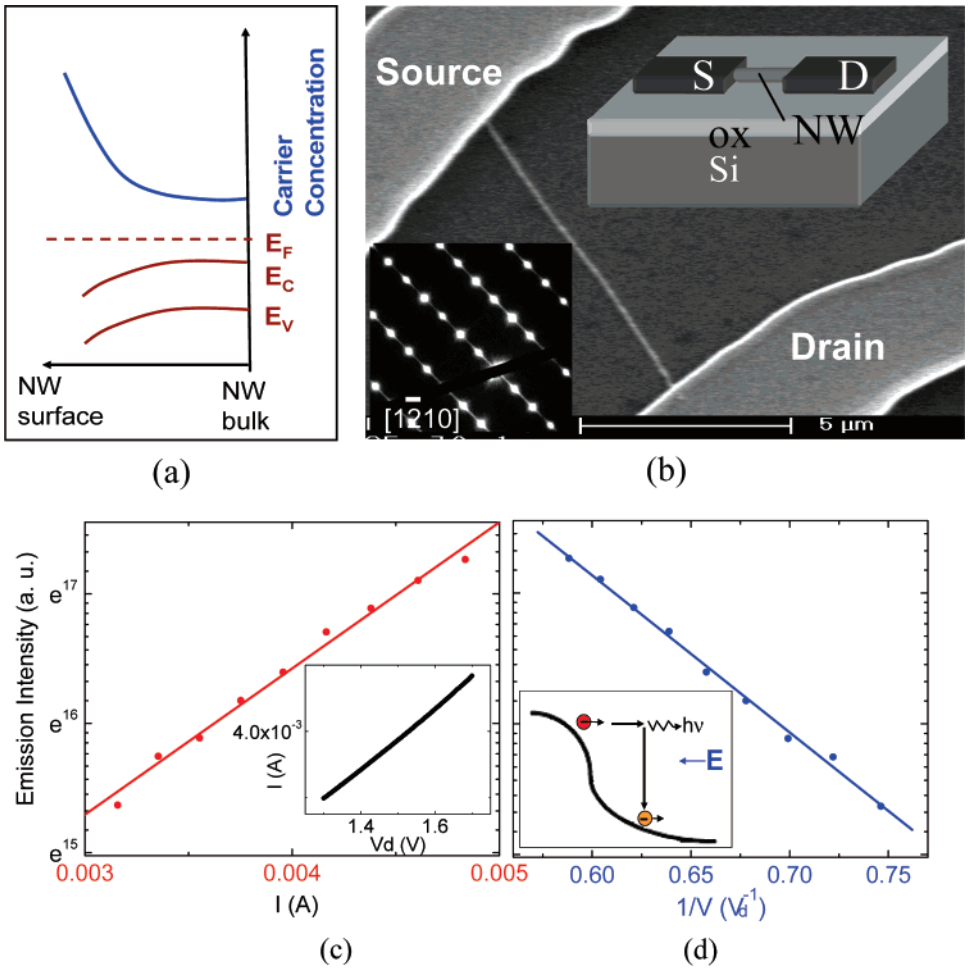

Figure 1. (a) Schematics of carrier distribution and band-bending along the radius of a highly doped InN NW; (b) An FE-SEM image of a representative InN NW device, and the inset shows a schematic of the back-gated FET configuration and a diffraction pattern; (c) Emission intensity vs drive current from an InN NW transistor, and the inset shows $I_d - V_d$; (d) Emission intensity vs $1/V_d$ from an InN NW transistor, and the inset shows a schematics of hot carrier emission.

valence-band maximum.[13,15] This means the surface Fermi level is 500−900 meV higher than the conduction-band minimum, implying a significant band bending at the surface. Instead of the depletion layer that is usually found on most other semiconductor surfaces,[17] an electron accumulation layer is formed on an InN surface and low resistance ohmic metal contacts to InN surfaces can be easily formed.[14] A schematic of the carrier distribution and band-bending along the radius of a highly doped InN NW is shown in Figure 1a, where both the carrier density and the band-bending are the highest on the NW surface.

The InN NWs used in this study were grown by a catalyst-free vapor−solid (VS) process.[18] A small quartz tube containing indium and indium oxide powders in a 1:1 ratio was loaded in the central part of a hot-wall CVD system. The tube was heated to 700 °C under Ar gas, then ammonia was introduced at a rate of 100 sccm for 30 min. The furnace was then adiabatically cooled to room temperature in an ammonia atmosphere. This growth procedure reproducibly led to a large deposition of NWs on the wall of the growth tube. The average NW lengths range from 3 to 30 μm and diameters from 70 to 150 nm. InN NWs harvested from the growth tube were suspended in isopropanol (IPA). The InN NW/IPA suspension was then dispersed onto a Si/SiO_2 wafer with previously fabricated vias to the substrate back gate. Source/drain pads to the NWs were defined by 50 nm Ni/200 nm Au. Figure 1b shows a field-emission scanning electron micrograph (FE-SEM) of such a single InN NW transistor and its device schematic in the inset. The single-crystal hexagonal wurtzite structure of the InN NWs was revealed by both HRTEM and diffraction patterns (inset of Figure 1b). In these devices, the drain current I_d increases monotonically with increasing gate voltage V_g, indicative of n-type material, as seen in bulk InN.[10] The carrier mobility μ of the transistor can then be calculated as:

$$\mu = (CV_{SD}/L^2)^{-1}(\partial I_{SD}/\partial V_{GD})|_{V_{SD}=1}$$

where $C = 2\pi\epsilon\epsilon_0 L/\ln(4h/d)$, L is the channel length, h is the SiO_2 thickness, d is the diameter of the NW, ϵ_0 is the vacuum permittivity, and ϵ is the dielectric constant of InN. The n-type InN NWs fabricated here had an average mobility of 29.2 ± 5.4 cm^2/Vs. Their carrier densities can be determined by $n = \sigma/e\mu$, and are in the range of $2.7 - 9 \times 10^{20}$ cm^{-3} in our samples. The large electron density is a result of

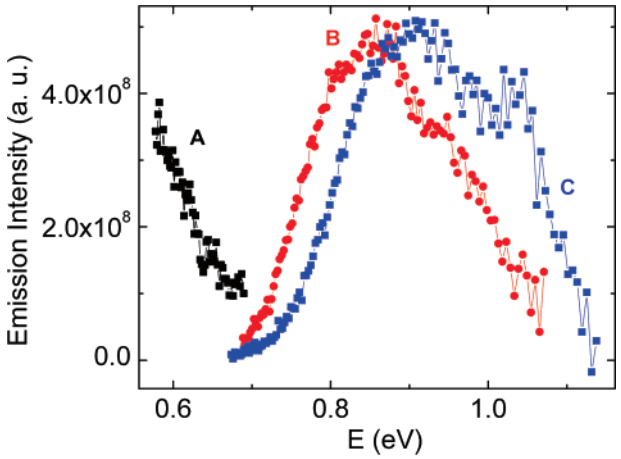

Figure 2. Emission spectrum from InN NW transistors using filters covering different wavelength ranges. The filter cutoff energy for curve A (sample B) is 0.58 eV, and the filter cutoff energy for curve B (sample B) and C (sample C) is 0.68 eV.

the surface electron accumulation layer, as discussed previously.[10,12−15]

Infrared (IR) electroluminescence (EL) from the InN NW transistors was imaged with a liquid nitrogen-cooled HgCdTe detector array mounted on the probe station, which was used to measure their electrical properties. The lateral resolution of the detector is diffraction-limited at about 2 μm. The EL was collected by a set of short-pass filters. The EL from an InN NW transistor is shown in Figure 3a, where both the total intensity and the emission spectrum can be recorded. We found that the emission intensity increases exponentially with drive current, while the current increases linearly with drain voltage, as shown in Figure 1c and its inset. This observation is similar to that reported in the case of single carbon nanotube emitters, where hot carriers impact−excite excitons under high electric field.[19,20] In our experiment, when an electron is accelerated to a sufficiently high energy under the high drain field ($\mathscr{E}$), and provided that it does not lose that energy by optical phonon scattering, it can create electron−hole pairs that then decay radiatively. The electron that lost energy to the generated exciton could in turn pick up energy from the field and continue this process. The probability for an electron to travel without scattering a distance l is given by $\exp(-l/\lambda_{ph})$, where λ_{ph} is the optical phonon scattering length. Therefore, the probability to accelerate an electron to energy E is $\sim \exp(-E/e\mathscr{E}\lambda_{ph})$, where e is the electron charge. The emission intensity generated by the high drain field $\mathscr{E}$ should be proportional to the impact excitation rate $\exp(-E/e\mathscr{E}\lambda_{ph}) = \exp(-EL/eV_d\lambda_{ph})$.[21] This agrees very well with what is observed experimentally: an exponential dependence between the emission intensity and the inverse of the drain field as shown in Figure 1d. The inset of Figure 1d shows a schematic of the impact excitation process discussed above.

To understand the origin of the InN NW EL, we measured the EL spectra, which are shown in Figure 2. We observed: (1) interband transition with a band gap of about 0.85 eV for sample B (curve B) and around 0.92 eV for sample C (curve C) (using a 1800 nm/0.67 eV short-pass (sp) filter in both cases), (2) hot-carrier intraband transition, curve A (sample B, below its band gap, using a 2200 nm/0.58 eV sp filter). This is the first time EL spectra of InN have been reported and the measured band gaps are very close to those obtained from photoluminescence (PL) (0.7−0.9 eV).[10−11] In both samples, we observed an additional peak around 80 meV higher than the main peak. The energy difference (80 meV) is very close to the longitudinal optical (LO) phonon energy in InN (73 meV),[10,22] suggesting the occurrence of phonon-assisted emission above the band gap. The emission below the band gap can be due to either Bremsstrahlung (ionized impurity-assisted) and/or phonon-assisted conduction-band to conduction-band emission,[23] and has *not* been observed in bulk InN PL spectroscopy before. The only relevant observation in the literature involves an exponentially decreasing weak absorption below the band gap.[24,25] In ionized impurity-assisted emissions, the intensity should depend linearly on the ionized impurity concentration and varies only weakly with carrier temperature and therefore is nearly independent of electrical field, whereas for phonon-assisted conduction-band to conduction-band emission, carrier temperature plays an important role.[23] Figure 3a gives the intensity of this IR emission at various drain biases. The emission intensity falls off exponentially with emitted photon energy. The higher the drain bias is, the "hotter" the carriers are. The strong dependence of the intensity on the drain field suggests a phonon-assisted origin. If we assume that the electrons obtain their energy by accelerating under the field E before being scattered by optical phonons, and that they equilibrate through e−e scattering (and their energy distribution can be characterized by an effective electron temperature), we then have $e\mathscr{E}\lambda_{ph} = k_B T_c$, where k_B is the Boltzmann's constant and T_c is the electron temperature. We can then estimate the temperature of the hot carriers in the InN NW (Figure 3) to be in the range of 900−1270 K as V_d is increased from 0.85 to 1 V.

The hot electrons relax further by emitting LO phonons. By calculating its energy-loss rate, we can obtain information into the carrier relaxation rate. Under a steady-state condition, the power lost through LO phonon emission is equal to the power provided to the electrons by the electric field:[26]

$$\frac{\hbar\omega_{LO}}{\tau}\exp\left(-\frac{\hbar\omega_{LO}}{k_B T_c}\right) = e\mu\mathscr{E}^2 \cong e\mu(V_d/L)^2$$

where ω_{LO} is the LO phonon frequency (73 meV)[27−28] and τ is the electron−LO phonon scattering time. Figure 3b shows that the inverse of the extracted carrier temperature T_c^{-1} varies linearly with $\ln(V_d^2)$, from which we can determine the e-ph scattering time to be approximately 200 fs, which agrees well with the results of Zanato et al.[22]

In our samples, which have carrier densities as high as 10^{21} cm^{-3} and the surface Fermi level is at 500−900 meV higher than the conduction-band minimum, we also need to consider the role of the Moss−Burstein effect on the optical transition energy.[10,26] The Pauli exclusion principle requires that the excited electrons must transit to unfilled states above or near the Fermi energy (E_F), therefore the valence band to

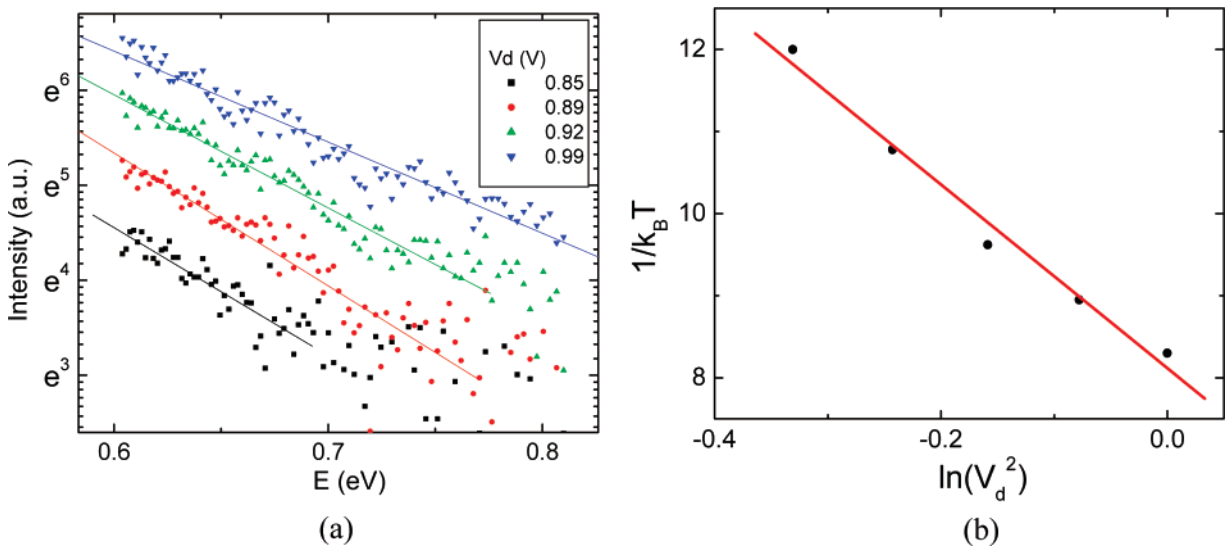

Figure 3. (a) Hot carrier emission from an InN NW transistor under various V_d biases. The straight lines are linear fits to the data; (b) $1/k_BT_c$ vs $\ln(V_d^2)$, with T_c extracted from Figure 3a. The straight line is a linear fit to the data.

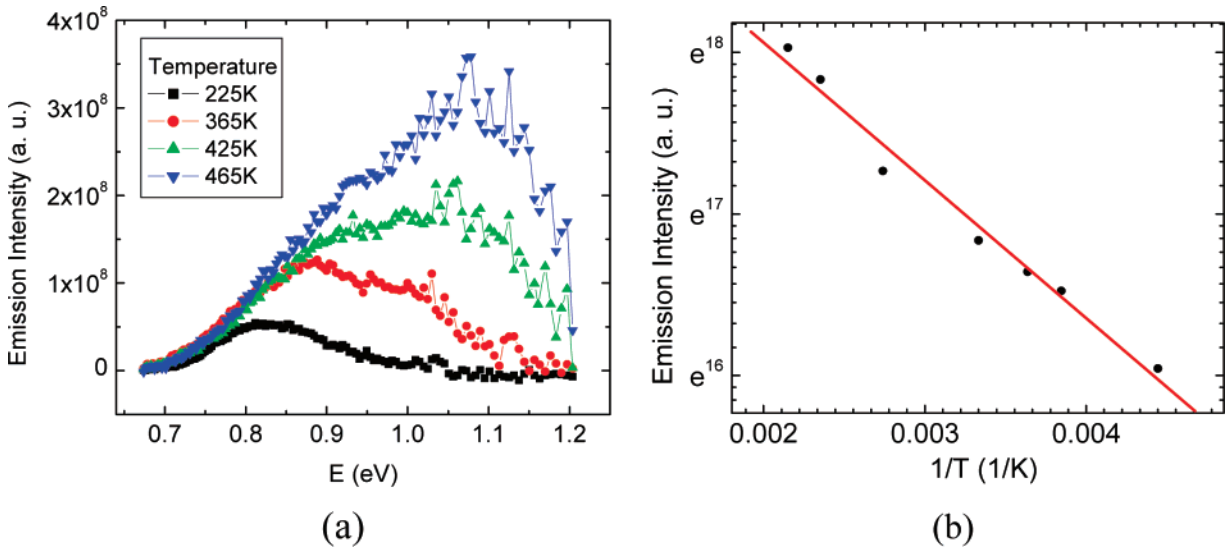

Figure 4. (a) Emission spectra from an InN NW under variable temperatures; (b) emission intensity vs $1/T$ from an InN NW, the straight line is a linear fit to the data.

conduction-band transition energy of an electron is increased by E_F. The corrected transition energy in a heavily doped sample is $E_g + E_F$. The fluctuation of carrier concentrations in our samples leads to a variation of the transition energies (from 0.85 to 0.92 eV), as shown in Figure 2. In a highly doped sample, conduction-band renormalization effects due to the electron−electron interaction and the electron-ionized impurity interaction[10,29] have to be considered. They become quite significant at higher electron concentrations, resulting in a red spectral shift of approximately 0.15 eV per decade of change of n beyond 10^{19} cm^{-3}.[23]

To further understand the interaction of phonons with the hot carriers in InN NWs, we measured the emission spectra at various temperatures. With decreasing temperature, the emission peak energy decreases, with around 0.8 mV/K, which is larger than the findings of PL experiments (0.2 mV/K).[11] Its temperature dependence is contrary to that of most direct band gap semiconductors, where a blue-shift in band gap is usually observed with decreasing temperature.[29] In general, PL emission is quenched at high temperatures because of increased nonradiative recombination processes.[10,11] On the contrary, here we observe a large *increase* in emission intensity with increasing temperature (Figure 4a). The intensity follows a $1/T$ dependence, with an activation barrier of 74 meV (Figure 4b), which coincides with the LO phonon energy and is close to the reported value for the electron-impurity binding energy, suggesting phonon-assisted hot-carrier emission.

The strongly accumulated surface electron layer generates a surface plasmon excitation whose frequency ω_{sp} is a function of the free carrier concentration ($\omega_{sp} \propto \sqrt{n}$).[16] Its detailed profile has been probed using high-resolution electron energy loss spectroscopy (HREELS) by Mahboob et al.[16] On the basis of their study, we extrapolated the plasma frequency for a sample with carrier concentration of

10^{22} cm^{-3} to be ~950 meV. At higher temperature, more carriers are activated to participate in the emission process via phonon-assisted processes and the increased carrier density shifts the peak ω_{sp} to higher energy. In an electroluminescent InN NW, plasmons can couple to the electron−hole pairs within its field penetration depth. The strongest coupling occurs near the plasmon resonance energy (ω_{sp}) where the plasmon density of states is high. This coupling could lead to an increased EL emission intensity. As the temperature is increased, ω_{sp} increases and the coupling results in an increased spectral weight of the emission at higher energy, i.e., a blue-shift at the emission. We note that the surfaces of our InN NWs are not perfectly flat, the average roughness is 20 nm, and the average grain size is approximately
120 nm. The roughness helps to scatter surface plasmons and allow them to couple to the light field. It the past, it has been shown in quantum wells and organic semiconductors that e−h pairs can couple efficiently with plasmons at a metal interface thus enhance PL intensity.[30−34] This unique property could lead to valuable applications in operating electroluminescent devices at elevated temperature.

In conclusion, we have successfully demonstrated for the first time EL in a single InN NW by impact excitation, measured its EL band gap, and observed interband and conduction-band to conduction-band hot-carrier emission. We propose that the surface plasmon formed from the electron accumulation layer at the InN NW surface enhances the radiative e−h recombination in InN.

Acknowledgment. We thank Dr. James Tsang for insightful discussions.

References

(1) Li, Y.; Qian, F.; Xiang, J.; Lieber, C. M. *Mater. Today* **2006**, *9*, 18.
(2) Huang, M. H.; Mao, S.; Feick, H.; Yan, H.; Wu, Y.; Kind, H.; Weber, E.; Russo, R.; Yang, P. *Science* **2001**, *292*, 1897.
(3) Duan, X.; Huang, Y.; Agarwal R.; Lieber, C. M. *Nature* **2003**, *421*, 241.
(4) Duan, X.; Huang, Y.; Cui, Y.; Wang, J.; Lieber, C. M. *Nature* **2001**, *409*, 66.
(5) Zhong, Z.; Qian, F.; Wang, D.; Lieber, C. M. *Nano Lett.* **2003**, *3*, 343.
(6) Qian, F.; Gradecak, S.; Li, Y.; Wen C.; Lieber, C. M. *Nano Lett.* **2005**, *5*, 2287.
(7) Huang, Y.; Dunn, X.; Lieber, C. M. *Small* **2005**, *1*, 142.
(8) Thelander, C.; Agarwal, P.; Brongersma, S.; Eymery, J.; Feiner, L. F.; Forchel, A.; Scheffler, M.; Riess, W.; Ohlsson, B. J.; Gosele, U.; Samuelson, L. *Mater. Today* **2006**, *9*, 28.
(9) Pauzauskie, P. J.; Yang, P. *Mater. Today* **2006**, *9*, 36.
(10) Bhuiyan, A.; Hashimoto, A.; Yamamoto, A. *J. Appl. Phys.* **2003**, *94*, 2779.
(11) Wu, J.; Walukiewicz, W.; Yu, K. M.; Ager, W. J., III; Haller, E. E.; Lu, H.; Schaff, W. J.; Saito, Y.; Nanishi, Y. *Appl. Phys. Lett.* **2002**, *80*, 3967.
(12) Mahboob, I.; Veal, T. D.; Piper, L. F. J.; McConville, C. F.; Lu, H.; Schaff, W. J.; Furthmuller, J.; Bechstedt, F. *Phys. Rev. B* **2004**, *69*, 201307.
(13) Veal, T. D.; Mahboob, I.; Piper, L. F. J.; McConville, C. F.; Lu, H.; Schaff, W. J. *J. Vac. Sci. Technol., B* **2004**, *22*, 2175
(14) Lu, H.; Schaff, W. J.; Eastman, L. F.; Stutz, C. E. *Appl. Phys. Lett.* **2003**, *82*, 1736
(15) Rickert, K. A.; Ellis, A. B.; Himpsel, F. J.; Lu, H.; Schaff, W. J.; Redwing, J. M.; Dwikusuma, F.; Kuech, T. F. *Appl. Phys. Lett.* **2003**, *82*, 3254.
(16) Mahboob, I.; Veal, T. D.; McConville, C. F.; Lu, H.; Schaff, W. J. *Phys. Rev. Lett.* **2004**, *92*, 036804.
(17) Calarco, R.; Marso, M.; Richter, T.; Aykanat, A. I.; Meijers, R.; V. D. Hart, A.; Stoica, T.; Luth, H. *Nano Lett.* **2005**, *5*, 981.
(18) Cheng, G.; Stern, E.; Turner-Evans, D.; Reed, M. A. *Appl. Phys. Lett.* **2005**, *87*, 253103.
(19) Chen, J.; Perebeios, V.; Freitag, M.; Tsang, J.; Fu, Q.; Liu, J.; Avouris, Ph.; *Science* **2005**, *310*, 1171.
(20) Perebeinos, V.; Avouris, Ph. *Phys. Rev. B* **2006**, *74*, 121410(R).
(21) Okuto, Y.; Crowell, C. R. *Phys. Rev. B* **1972**, *6*, 3076.
(22) Zanato, D.; Balkan, N.; Ridley, B. K.; Hill, G.; Schaff, W. J. *Semicond. Sci. Technol.* **2004**, *19*, 1024.
(23) Onodera K.; Nishimura, K.; Furuta, T. *IEEE Trans. Electron. Devices* **1999**, *46*, 2170.
(24) Butcher, K. S. A.; Hirshy, H.; Perks, R. M.; Wintrebert-Fouquet, M.; Chen, P. P-T. *Phys. Status Solidi A* **2006**, *203*, 66.
(25) Shubina, T. V.; Ivanov, S. V.; Jmerik, V. N.; Toropov, A. A.; Vasson, A.; Leymarie, J.; Kop'ev, P. S. *Phys. Status Solidi A* **2006**, *203*, 13.
(26) Ridley, B. K. *Quantum Processes in Semiconductors*; Oxford University Press: London, 1982.
(27) Kasic, A.; Schubert, M.; Saito, Y.; Nanishi, Y.; Wagner, G. *Phys. Rev. B* **2002**, *65*, 115206.
(28) Inushima, T.; Higashiwaki, M.; Matsui, T. *Phys. Rev. B* **2003**, *68*, 235204.
(29) Walukiewicz, W. *Phys. Rev. B* **1990**, *41*, 10218.
(30) Yu, V.; Davydov, V.; Emtsev, V.; Goncharuk, I. N.; Smirnov, A. N.; Petrikov, V. D.; Mamutin, V. V.; Vekshin, V. A.; Ivanov, S. V. *Appl. Phys. Lett.* **1999**, *75*, 3297.
(31) Shan, W.; Schmidt, T. J.; Yang, X. H.; Hwang, S. K.; Song, J. J.; Goldenberg, B. *Appl. Phys. Lett.* **1995**, *66*, 985.
(32) Okamoto, K.; Niki, I.; Shvartser, A.; Narukawa, Y.; Mukai, T.; Scherer, A. *Nat. Mater.* **2004**, *3*, 601.
(33) Hecker, N. E.; Höpfel, R. A.; Sawaki, N.; Maier, T.; Strasser, G. *Appl. Phys. Lett.* **1999**, *75*, 1577.
(34) Bellessa, J.; Bonnand, C.; Plenet, J. C.; Mugnier, J. *Phys. Rev. Lett.* **2004**, *93*, 036404.

NL070852Y